

CERN-TH/98-1  
 UCHEP-98/7  
 hep-ph/9803368

# Direct CP Violation in $B \rightarrow X_s \gamma$ Decays as a Signature of New Physics

Alexander L. Kagan

*Department of Physics, University of Cincinnati  
 Cincinnati, Ohio 45221, USA*

and

Matthias Neubert

*Theory Division, CERN, CH-1211 Geneva 23, Switzerland*

## Abstract

We argue that the observation of a sizable direct CP asymmetry  $A_{\text{CP}}^{b \rightarrow s\gamma}$  in the inclusive decays  $B \rightarrow X_s \gamma$  would be a clean signal of New Physics. In the Standard Model,  $A_{\text{CP}}^{b \rightarrow s\gamma}$  can be calculated reliably and is found to be below 1% in magnitude. In extensions of the Standard Model with new CP-violating couplings, large CP asymmetries are possible without conflicting with the experimental value of the branching ratio for the decays  $B \rightarrow X_s \gamma$ . In particular, large asymmetries arise naturally in models with enhanced chromo-magnetic dipole operators. Some generic examples of such models are explored and their implications for the semileptonic branching ratio and charm yield in  $B$  decays discussed.

(Submitted to Physical Review D)

CERN-TH/98-1  
 March 1998

# 1 Introduction

Studies of rare decays of  $B$  mesons have the potential to uncover the origin of CP violation, which may lie outside the Standard Model of strong and electroweak interactions. The measurements of several asymmetries will make it possible to test whether the CKM mechanism of CP violation is sufficient, or whether additional sources of CP violation are required to describe the data. In order to achieve this goal, it is necessary that the theoretical calculations of CP-violating observables in terms of Standard Model parameters are, at least to a large extent, free of hadronic uncertainties. This can be achieved, for instance, by measuring time-dependent asymmetries in the decays of neutral  $B$  mesons into particular CP eigenstates. In many other cases, however, the theoretical predictions for direct CP violation in exclusive  $B$  decays are obscured by large strong-interaction effects [1]–[4], which can only partly be controlled using the approximate flavour symmetries of QCD [5].

Inclusive decay rates of  $B$  mesons, on the other hand, can be reliably calculated in QCD using the operator product expansion. Up to small bound-state corrections these rates agree with the parton model predictions for the underlying decays of the  $b$  quark [6]–[8]. The possibility of observing mixing-induced CP asymmetries in inclusive decays of neutral  $B$  mesons has been emphasized in Ref. [9]. The disadvantage that the inclusive sum over many final states partially dilutes the asymmetries is compensated by the fact that, because of the short-distance nature of inclusive processes, the strong phases are calculable using quark–hadron duality. The resulting CP asymmetries are proportional to the strong coupling constant  $\alpha_s(m_b)$ . The purpose of the present paper is to study direct CP violation in the rare radiative decays  $B \rightarrow X_s \gamma$ , both in the Standard Model and beyond. These decays have already been observed experimentally, and copious data samples will be collected at the  $B$  factories. As long as the fine structure of the photon energy spectrum is not probed locally, the theoretical analysis relies only on the weak assumption of global quark–hadron duality (unlike the hadronic inclusive decays considered in Ref. [9]). Also, the leading nonperturbative corrections have been studied in detail and are well understood [10]–[17].

We perform a model-independent analysis of CP-violating effects in  $B \rightarrow X_s \gamma$  decays in terms of the effective Wilson coefficients  $C_7 \equiv C_7^{\text{eff}}(m_b)$  and  $C_8 \equiv C_8^{\text{eff}}(m_b)$  multiplying the (chromo-) magnetic dipole operators

$$O_7 = \frac{e m_b}{4\pi^2} \bar{s}_L \sigma_{\mu\nu} F^{\mu\nu} b_R, \quad O_8 = \frac{g_s m_b}{4\pi^2} \bar{s}_L \sigma_{\mu\nu} G^{\mu\nu} b_R \quad (1)$$

in the low-energy effective weak Hamiltonian [18]. We will allow for generic New Physics contributions to the coefficients  $C_7$  and  $C_8$ , possibly containing new CP-violating couplings. Several extensions of the Standard Model in which new contributions to dipole operators arise have been explored, e.g., in Refs. [19, 20]. We find that in the Standard Model the direct CP asymmetry in the decays  $B \rightarrow X_s \gamma$  is very small (below 1% in magnitude) because of a combination of CKM and GIM suppression, both of which can be lifted in extensions of the Standard Model. If there are new contributions to the dipole operators with sizable weak phases, they can induce a CP asymmetry that is

more than an order of magnitude larger than in the Standard Model. We thus propose a measurement of the inclusive CP asymmetry in the decays  $B \rightarrow X_s \gamma$  as a clean and sensitive probe of New Physics. For simplicity, we shall not consider here the most general scenario of having other, non-standard operators in the effective Hamiltonian. However, we will discuss the important case of new dipole operators involving right-handed light-quark fields, which occur, for instance, in left-right symmetric models. The interference of these operators with those of the standard basis, which is necessary for CP violation, is strongly suppressed by a power of  $m_s/m_b$ ; still, they can give sizable contributions to CP-averaged branching ratios for rare  $B$  decays.

Studies of direct CP violation in the inclusive decays  $B \rightarrow X_s \gamma$  have been performed previously by several authors, both in the Standard Model [21] and in certain extensions of it [22, 23]. In all cases, rather small asymmetries of order a few percent or less are obtained. Here, we generalize and extend these analyses in various ways. Besides including some contributions to the asymmetry neglected in previous works, we shall investigate in detail a class of New Physics models with enhanced chromo-magnetic dipole contributions, in which large CP asymmetries of order 10–50% are possible and even natural. We also perform a full next-to-leading order analysis of the CP-averaged  $B \rightarrow X_s \gamma$  branching ratio in order to derive constraints on the parameter space of the New Physics models considered here. For completeness, we note that CP violation has also been studied in the related decays  $B \rightarrow X_s \ell^+ \ell^-$  [24], which however have a much smaller branching ratio than the radiative decays considered here.

## 2 Direct CP violation in radiative $B$ decays

The starting point in the calculation of the inclusive  $B \rightarrow X_s \gamma$  decay rate is provided by the effective weak Hamiltonian renormalized at the scale  $\mu = m_b$  [18]. Direct CP violation in these decays may arise from the interference of non-trivial weak phases, contained in CKM matrix elements or in possible New Physics contributions to the Wilson coefficient functions, with strong phases provided by the imaginary parts of the matrix elements of the local operators of the effective Hamiltonian [25]. These imaginary parts first arise at  $O(\alpha_s)$  from loop diagrams containing charm quarks, light quarks or gluons. Using the formulae of Greub et al. for these contributions [26], we calculate at next-to-leading order the difference  $\Delta\Gamma = \Gamma(\bar{B} \rightarrow X_s \gamma) - \Gamma(B \rightarrow X_{\bar{s}} \gamma)$  of the CP-conjugate, inclusive decay rates. The contributions to  $\Delta\Gamma$  from virtual corrections arise from interference of the one-loop diagrams with insertions of the operators  $O_2$  and  $O_8$  shown in Figure 1(a) and (b) with the tree-level diagram for  $b \rightarrow s \gamma$  containing an insertion of the operator  $O_7$ . Here  $O_2 = \bar{s}_L \gamma_\mu q_L \bar{q}_L \gamma^\mu b_L$  with  $q = c, u$  are the usual current–current operators in the effective Hamiltonian. We find

$$\begin{aligned} \Delta\Gamma_{\text{virt}} &= \frac{G_F^2 m_b^5 \alpha \alpha_s(m_b)}{18\pi^4} \\ &\times \left\{ -\frac{5}{9} \text{Im}[v_u v_t^* C_2 C_7^*] - \left( \frac{5}{9} - z v(z) \right) \text{Im}[v_c v_t^* C_2 C_7^*] - \frac{|v_t|^2}{2} \text{Im}[C_8 C_7^*] \right\}, \quad (2) \end{aligned}$$

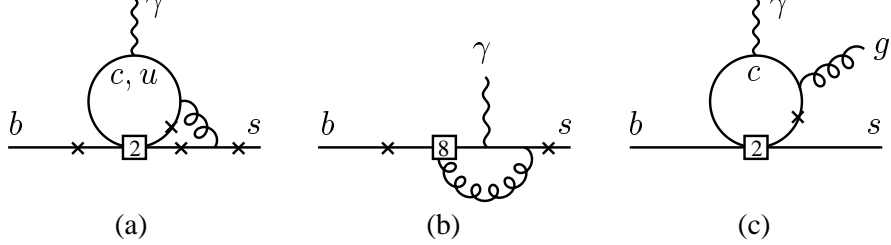


Figure 1: Diagrams for  $b \rightarrow s\gamma(g)$  yielding non-trivial strong phases that can contribute to the CP asymmetry. The crosses indicate other possible attachments of the photon. The numbers inside the squares indicate which operators are inserted.

where  $v_q = V_{qs}^* V_{qb}$  are products of CKM matrix elements,  $z = (m_c/m_b)^2$ , and

$$v(z) = \left(5 + \ln z + \ln^2 z - \frac{\pi^2}{3}\right) + \left(\ln^2 z - \frac{\pi^2}{3}\right)z + \left(\frac{28}{9} - \frac{4}{3} \ln z\right)z^2 + O(z^3). \quad (3)$$

There are also contributions to  $\Delta\Gamma$  from gluon bremsstrahlung diagrams with a charm-quark loop, shown in Figure 1(c). They can interfere with the tree-level diagrams for  $b \rightarrow s\gamma g$  containing an insertion of  $O_7$  or  $O_8$ . Contrary to the virtual corrections, for which in the parton model the photon energy is fixed to its maximum value, the gluon bremsstrahlung diagrams lead to a non-trivial photon spectrum, and so the results depend on the experimental lower cutoff on the photon energy. We define a quantity  $\delta$  by the requirement that  $E_\gamma > (1 - \delta)E_\gamma^{\max}$ , i.e.  $\delta$  is the fraction of the spectrum above the cut.<sup>1</sup> We then obtain

$$\Delta\Gamma_{\text{brems}} = \frac{G_F^2 m_b^5 \alpha \alpha_s(m_b)}{18\pi^4} z b(z, \delta) \left( \text{Im}[v_c v_t^* C_2 C_7^*] - \frac{1}{3} \text{Im}[v_c v_t^* C_2 C_8^*] \right), \quad (4)$$

where  $b(z, \delta) = g(z, 1) - g(z, 1 - \delta)$  with

$$g(z, y) = \theta(y - 4z) \left\{ (y^2 - 4yz + 6z^2) \ln \left( \sqrt{\frac{y}{4z}} + \sqrt{\frac{y}{4z} - 1} \right) - \frac{3y(y - 2z)}{4} \sqrt{1 - \frac{4z}{y}} \right\}. \quad (5)$$

Combining the two contributions, dividing the result by the leading-order expression for (twice) the CP-averaged inclusive decay rate,

$$\Gamma(\bar{B} \rightarrow X_s \gamma) + \Gamma(B \rightarrow X_{\bar{s}} \gamma) = \frac{G_F^2 m_b^5 \alpha}{16\pi^4} |v_t C_7|^2, \quad (6)$$

and using the unitarity relation  $v_u + v_c + v_t = 0$ , we find for the CP asymmetry

$$A_{\text{CP}}^{b \rightarrow s\gamma}(\delta) = \frac{\Gamma(\bar{B} \rightarrow X_s \gamma) - \Gamma(B \rightarrow X_{\bar{s}} \gamma)}{\Gamma(\bar{B} \rightarrow X_s \gamma) + \Gamma(B \rightarrow X_{\bar{s}} \gamma)} \Big|_{E_\gamma > (1 - \delta)E_\gamma^{\max}}$$

<sup>1</sup>In the parton model  $E_\gamma^{\max} = m_b/2$  depends on the quark mass and does not agree with the physical boundary of phase space. Later, we shall discuss how this problem is resolved by including the effects of Fermi motion.

$$\begin{aligned}
&= \frac{\alpha_s(m_b)}{|C_7|^2} \left\{ \frac{40}{81} \text{Im}[C_2 C_7^*] - \frac{8z}{9} [v(z) + b(z, \delta)] \text{Im}[(1 + \epsilon_s) C_2 C_7^*] \right. \\
&\quad \left. - \frac{4}{9} \text{Im}[C_8 C_7^*] + \frac{8z}{27} b(z, \delta) \text{Im}[(1 + \epsilon_s) C_2 C_8^*] \right\}, \tag{7}
\end{aligned}$$

where

$$\epsilon_s = \frac{v_u}{v_t} = \frac{V_{us}^* V_{ub}}{V_{ts}^* V_{tb}} \approx \lambda^2(i\eta - \rho) = O(10^{-2}). \tag{8}$$

In the last step, we have expressed  $\epsilon_s$  in terms of the Wolfenstein parameters, with  $\lambda = \sin \theta_C \approx 0.22$  and  $\rho, \eta = O(1)$ . We stress that (7) is an exact next-to-leading order result. All numerical coefficients are independent of the renormalization scheme. For consistency, the ratios of Wilson coefficients  $C_i$  must be evaluated in leading-logarithmic order. Whereas the bremsstrahlung contributions as well as the  $C_2$ – $C_8$  interference term are new, an estimate of the  $C_2$ – $C_7$  interference term has been obtained previously by Soares [21], who neglects the contribution of the function  $b(z, \delta)$  and uses an approximation for  $v(z)$ . The importance of the  $C_8$ – $C_7$  interference term for certain extensions of the Standard Model has been stressed by Wolfenstein and Wu [22], and the first correct calculation of its coefficient can be found in Ref. [23].

In the Standard Model, the Wilson coefficients take the real values  $C_2 \approx 1.11$ ,  $C_7 \approx -0.31$  and  $C_8 \approx -0.15$ . The imaginary part of the small quantity  $\epsilon_s$  is thus the only source of CP violation. Note that all terms involving this quantity are GIM suppressed by a power of the small ratio  $z = (m_c/m_b)^2$ , reflecting the fact that there is no non-trivial weak phase difference in the limit where  $m_c = m_u = 0$ . Hence, the Standard Model prediction for the CP asymmetry is suppressed by three small factors:  $\alpha_s(m_b)$  arising from the strong phases,  $\sin^2 \theta_C$  reflecting the CKM suppression, and  $(m_c/m_b)^2$  resulting from the GIM suppression. The numerical result for the CP asymmetry depends on the values of the strong coupling constant and the ratio of the heavy-quark pole masses. Throughout this work we shall take  $\alpha_s(m_b) \approx 0.214$  (corresponding to  $\alpha_s(m_Z) = 0.118$  and two-loop evolution down to the scale  $m_b = 4.8$  GeV) and  $\sqrt{z} = m_c/m_b = 0.29$ . The sensitivity of the next-to-leading order predictions for inclusive  $B$  decay rates to theoretical uncertainties in the values of the input parameters as well as to the choice of the renormalization scale and scheme have been investigated by several authors. Typically, the resulting uncertainties are of the order of 10%. Since a discussion of such effects is not the purpose of our study, we shall for simplicity assume fixed values of the input parameters as quoted above. With this choice we find

$$A_{\text{CP,SM}}^{b \rightarrow s\gamma}(\delta) \approx 1.54\% [1 + 0.15 b(z, \delta)] \eta, \tag{9}$$

where  $0 \leq b(z, \delta) < 0.30$  depending on the value of  $\delta$ . With  $\eta \approx 0.2$ – $0.4$  as suggested by phenomenological analyses [27], we find a tiny asymmetry of about 0.5%, in agreement with the estimate obtained in Ref. [21]. Expression (7) applies also to the decays  $B \rightarrow X_d \gamma$ , the only difference being that in this case the quantity  $\epsilon_s$  must be replaced with

the corresponding quantity

$$\epsilon_d = \frac{V_{ud}^* V_{ub}}{V_{td}^* V_{tb}} \approx \frac{\rho - i\eta}{1 - \rho + i\eta} = O(1). \quad (10)$$

Therefore, in the Standard Model the CP asymmetry in  $B \rightarrow X_d \gamma$  decays is larger by a factor  $-(\lambda^2[(1 - \rho)^2 + \eta^2])^{-1} \approx -20$  than that in  $B \rightarrow X_s \gamma$  decays. Note, however, that experimentally it would be very difficult to distinguish between inclusive  $B \rightarrow X_s \gamma$  and  $B \rightarrow X_d \gamma$  decays. If only the sum is measured, the CP asymmetry vanishes (in the limit where  $m_s = m_d = 0$ ), since

$$\Delta\Gamma_{\text{SM}}(B \rightarrow X_s \gamma) + \Delta\Gamma_{\text{SM}}(B \rightarrow X_d \gamma) \propto \text{Im}[V_{ub} V_{tb}^* (V_{us}^* V_{ts} + V_{ud}^* V_{td}^*)] = 0 \quad (11)$$

by unitarity.

From (7) it is apparent that two of the suppression factors operative in the Standard Model,  $z$  and  $\lambda^2$ , can be avoided in models where the effective Wilson coefficients  $C_7$  and  $C_8$  receive additional contributions involving non-trivial weak phases. Much larger CP asymmetries of  $O(\alpha_s)$  then become possible. In order to investigate such models, we may to good approximation neglect the small quantity  $\epsilon_s$  and write

$$A_{\text{CP}}^{b \rightarrow s \gamma}(\delta) = \frac{1}{|C_7|^2} \left\{ a_{27}(\delta) \text{Im}[C_2 C_7^*] + a_{87} \text{Im}[C_8 C_7^*] + a_{28}(\delta) \text{Im}[C_2 C_8^*] \right\}, \quad (12)$$

where

$$a_{27}^{(\text{p})}(\delta) = \alpha_s(m_b) \left\{ \frac{40}{81} - \frac{8z}{9} [v(z) + b(z, \delta)] \right\},$$

$$a_{87}^{(\text{p})} = -\frac{4}{9} \alpha_s(m_b), \quad a_{28}^{(\text{p})}(\delta) = \frac{8}{27} \alpha_s(m_b) z b(z, \delta). \quad (13)$$

The superscripts indicate that these results are obtained in the parton model. The values of the coefficients  $a_{ij}^{(\text{p})}$  are shown in the left portion of Table 1 for three choices of the cutoff on the photon energy:  $\delta = 1$  corresponding to the (unrealistic) case of a fully inclusive measurement,  $\delta = 0.3$  corresponding to a restriction to the part of the spectrum above  $\approx 1.8$  GeV, and  $\delta = 0.15$  corresponding to a cutoff that removes almost all of the background from  $B$  decays into charmed hadrons. In practice, a restriction to the high-energy part of the photon spectrum is required for experimental reasons. Whereas the third term in (12) will generally be very small, the first two terms can give rise to sizable effects. Since  $a_{27}^{(\text{p})}$  has a rather weak dependence on  $\delta$  and  $a_{87}^{(\text{p})}$  has none, the result for the CP asymmetry is not very sensitive to the choice of the photon-energy cutoff. Assume now that there is a New Physics contribution to  $C_7$  of similar magnitude as the Standard Model contribution, so as not to spoil the prediction for the CP-averaged decay rate in (6), but with a non-trivial weak phase. Then the first term in (12) may give a contribution of up to about 5% in magnitude. Similarly, if there are New Physics contributions to  $C_7$  and  $C_8$  such that the ratio  $C_8/C_7$  has a non-trivial weak phase, the

Table 1: Values of the coefficients  $a_{ij}$  (in %), without (left) and with (right) Fermi motion effects included

$\delta$	$a_{27}^{(p)}$	$a_{87}^{(p)}$	$a_{28}^{(p)}$	$a_{27}$	$a_{87}$	$a_{28}$	$E_\gamma^{\min}$ [GeV]
	(parton model)			(with Fermi motion)			
1.00	1.06	-9.52	0.16	1.06	-9.52	0.16	0.00
0.30	1.17	-9.52	0.12	1.23	-9.52	0.10	1.85
0.15	1.31	-9.52	0.07	1.40	-9.52	0.04	2.24

second term may give a contribution of up to about  $10\% \times |C_8/C_7|$ . In models with a strong enhancement of  $|C_8|$  with respect to its Standard Model value, there is thus the possibility of generating very large CP asymmetries in  $B \rightarrow X_s \gamma$  decays. The relevance of the second term for two-Higgs-doublet models, and for left-right symmetric extensions of the Standard Model, has been explored in Refs. [22, 23].

In our discussion so far we have neglected nonperturbative power corrections to the inclusive decay rates. Their impact on the rate ratio defining the CP asymmetry is expected to be very small, since most of the corrections will cancel between the numerator and the denominator. Potentially the most important bound-state effect is the Fermi motion of the  $b$  quark inside the  $B$  meson, which determines the shape of the photon energy spectrum in the endpoint region. Technically, Fermi motion is included in the heavy-quark expansion by resumming an infinite set of leading-twist corrections into a nonperturbative ‘‘shape function’’  $F(k_+)$ , which governs the light-cone momentum distribution of the heavy quark inside the meson [11, 12]. The physical decay distributions are obtained from a convolution of parton model spectra with this function. In the process, phase-space boundaries defined by parton model kinematics are transformed into the proper physical boundaries defined by hadron kinematics. For the particular case of the coefficients  $a_{ij}^{(p)}(\delta)$  in (13), where in the parton model the parameter  $\delta$  is defined such that  $E_\gamma \geq \frac{1}{2}(1-\delta)m_b$ , it can be shown that the physical coefficients  $a_{ij}(\delta)$  with  $E_\gamma \geq \frac{1}{2}(1-\delta)m_B$  are given by [28]

$$a_{ij}(\delta) = \frac{\int_{m_B(1-\delta)-m_b}^{m_B-m_b} dk_+ F(k_+) a_{ij}^{(p)}\left(1 - \frac{m_B(1-\delta)}{m_b+k_+}\right)}{\int_{m_B(1-\delta)-m_b}^{m_B-m_b} dk_+ F(k_+)} . \quad (14)$$

This relation is such that there is no effect if either the parton model coefficient is independent of  $\delta$ , or if the limit  $\delta = 1$  is taken, i.e. the restriction on the photon energy is removed. Several ansätze for the shape function have been suggested in the literature [11, 12]. For our purposes, it is sufficient to adopt the simple form

$$F(k_+) = N(1-x)^a e^{(1+a)x}; \quad x = \frac{k_+}{\Lambda} \leq 1, \quad (15)$$

where  $\bar{\Lambda} = m_B - m_b$ . The normalization  $N$  cancels in the ratio in (14). The parameter  $a$  can be related to the heavy-quark kinetic energy parameter  $\mu_\pi^2 = -\lambda_1$  [29], yielding  $\mu_\pi^2 = 3\bar{\Lambda}^2/(1+a)$ . In the right portion of Table 2, we show the values of the coefficients  $a_{ij}(\delta)$  corrected for Fermi motion, using the above ansatz with  $m_b = 4.8 \text{ GeV}$  and  $\mu_\pi^2 = 0.3 \text{ GeV}^2$ . We also give the physical values of the minimum photon energy,  $E_\gamma^{\min} = \frac{1}{2}(1-\delta)m_B$ . The largest coefficient,  $a_{87}$ , is not affected by Fermi motion, and the impact on the other two coefficients is rather mild. As a consequence, our predictions for the CP asymmetry are very much insensitive to bound-state effects, even if a restriction on the high-energy part of the photon spectrum is imposed.

### 3 Next-to-leading order corrections to $B \rightarrow X_s \gamma$

In the next section we shall explore in detail the structure of New Physics models with a potentially large inclusive CP asymmetry. A non-trivial constraint on such models is that they must yield an acceptable result for the total, CP-averaged  $B \rightarrow X_s \gamma$  branching ratio, which has been measured experimentally. Taking a weighed average of the results reported by the CLEO and ALEPH Collaborations [30, 31] gives  $B(B \rightarrow X_s \gamma) = (2.6 \pm 0.6) \times 10^{-4}$ . We stress that this value is extracted from a measurement of the high-energy part of the photon energy spectrum assuming that the shape of the spectrum is as predicted by the Standard Model. For instance, the CLEO Collaboration has measured the spectrum in the energy range between 2.2 and 2.7 GeV and applied a correction factor of  $0.82 \pm 0.06$  in order to extrapolate to the total decay rate [32] (see Ref. [28] for a critical discussion of this treatment).

The complete theoretical prediction for the  $B \rightarrow X_s \gamma$  decay rate at next-to-leading order has been presented for the first time by Chetyrkin et al. [33]. The result for the corresponding branching ratio is usually obtained by normalizing the radiative decay rate to the semileptonic decay rate of  $B$  mesons, thus eliminating the strong dependence on the  $b$ -quark mass. We define

$$\frac{\Gamma(B \rightarrow X_s \gamma)|_{E_\gamma > (1-\delta)E_\gamma^{\max}}}{\Gamma(B \rightarrow X_c e \bar{\nu})} = \frac{6\alpha}{\pi f(z)} \left| \frac{V_{ts}^* V_{tb}}{V_{cb}} \right|^2 K_{\text{NLO}}(\delta), \quad (16)$$

where  $f(z) = 1 - 8z + 8z^3 - z^4 - 12z^2 \ln z$  is a phase-space factor, and the quantity  $K_{\text{NLO}}(\delta) = |C_7|^2 + O(\alpha_s, 1/m_b^2)$  contains the corrections to the leading-order result. Using  $\alpha^{-1} = \alpha(m_b)^{-1} \approx 130.3$  and  $|V_{ts}^* V_{tb}/V_{cb}| \approx 0.976$  as in Ref. [33], we get

$$B(B \rightarrow X_s \gamma)|_{E_\gamma > (1-\delta)E_\gamma^{\max}} \approx 2.705 \times 10^{-3} K_{\text{NLO}}(\delta) \times \frac{B(B \rightarrow X_c e \bar{\nu})}{10.5\%}. \quad (17)$$

From now on we shall assume the value  $B(B \rightarrow X_c e \bar{\nu}) = 10.5\%$  for the semileptonic branching ratio and omit the last factor. The current experimental situation of measurements of this quantity and their theoretical interpretation are reviewed in Refs. [34, 35].

Table 2: Values of the coefficients  $k_{ij}$  (in %) with Fermi motion effects included

$\delta$	$E_\gamma^{\min}$ [GeV]	$k_{77}$	$k_{22}$	$k_{88}$	$k_{27}$	$k_{78}$	$k_{28}$	$k_{77}^{(1)}$
0.99	0.03	76.42	0.23	21.35	-14.53	9.36	-0.04	3.41
0.30	1.85	68.13	0.11	0.53	-16.55	8.85	-0.01	3.86
0.15	2.24	52.18	0.03	0.11	-13.54	6.66	+0.00	3.15

The general structure of the quantity  $K_{\text{NLO}}$  is

$$K_{\text{NLO}}(\delta) = \sum_{\substack{i,j=2,7,8 \\ i \leq j}} k_{ij}(\delta) \text{Re}[C_i C_j^*] + k_{77}^{(1)}(\delta) \text{Re}[C_7^{(1)} C_7^*], \quad (18)$$

where  $k_{ij}(\delta)$  are known coefficient functions depending on the energy cutoff parameter  $\delta$ , and  $C_7^{(1)}$  is the next-to-leading order contribution to the Wilson coefficient  $C_7^{\text{eff}}(m_b)$ . In the Standard Model  $C_7^{(1)} \approx 0.48$  [33]. Explicit expressions for the functions  $k_{ij}(\delta)$ , at next-to-leading order in  $\alpha_s$  and including power corrections of order  $1/m_b^2$ , can be found in Ref. [28], where we correct some mistakes in the formulae used by previous authors. (The corrected expressions will also be given in an erratum to Ref. [33].) Contrary to the case of the CP asymmetry, the impact of Fermi motion on the partially integrated  $B \rightarrow X_s \gamma$  decay rate is an important one for values of  $\delta$  that are realistic for present-day experiments. In Table 2, we show the values of the coefficients  $k_{ij}$  corrected for Fermi motion [28], using again  $m_b = 4.8$  GeV and  $\mu_\pi^2 = 0.3$  GeV $^2$  for the parameters of the shape function. We quote the results for three choices of the cutoff on the photon energy:  $\delta = 0.99$  corresponding to a “fully” inclusive measurement, and  $\delta = 0.3$  and  $0.15$  corresponding to a restriction to the high-energy part of the photon spectrum. The choice  $\delta = 1$  must be avoided because of a weak, logarithmic soft-photon divergence in the prediction for the total  $B \rightarrow X_s \gamma$  branching ratio caused by the term proportional to  $k_{88}(\delta)$ . Note that with a realistic choice of the cutoff parameter  $\delta$  the coefficient  $k_{88}$  of the term proportional to  $|C_8|^2$  in (18) becomes very small. This observation will become important later on. With our choice of parameters, we obtain in the Standard Model  $B(B \rightarrow X_s \gamma) = (3.59 \pm 0.29) \times 10^{-4}$  for  $\delta = 0.99$  [28], in good agreement with the results obtained in previous analyses [33, 36, 37].

In order to illustrate the sensitivity of our results to the parameters of the shape function, we show in Figure 2 the predictions for the Standard Model branching ratio as a function of the energy cutoff  $E_\gamma^{\min} = \frac{1}{2}(1-\delta)m_B$ . In the first plot, we keep  $m_b = 4.8$  GeV fixed and compare the parton model result (gray curve) with the results corrected for Fermi motion, using  $\mu_\pi^2 = 0.15$  GeV $^2$  (short-dashed curve), 0.30 GeV $^2$  (solid curve), and 0.45 GeV $^2$  (long-dashed curve). This figure illustrates how Fermi motion fills the gap between the parton model endpoint at  $m_b/2$  and the physical endpoint<sup>2</sup> at  $m_B/2$ . In

<sup>2</sup>The true physical endpoint is actually located at  $(m_B^2 - m_{K^*}^2)/2m_B \approx 2.56$  GeV, i.e. slightly below

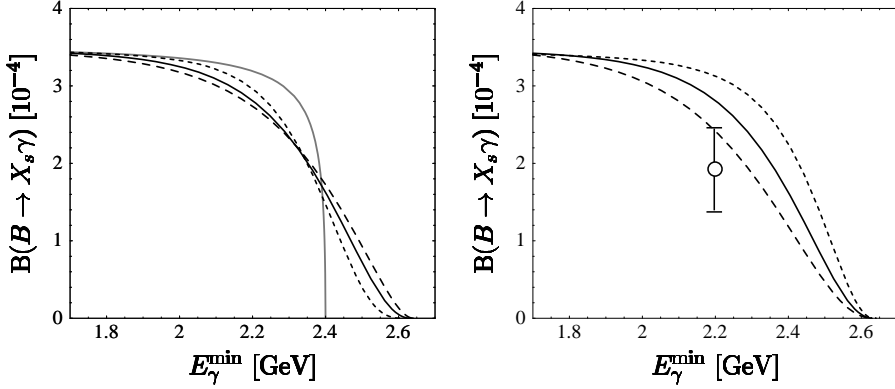


Figure 2: *Theoretical predictions for the integrated  $B \rightarrow X_s\gamma$  branching ratio for various choices of the parameters  $m_b$  and  $\mu_\pi^2$ ; left:  $\mu_\pi^2 = (0.30 \pm 0.15) \text{ GeV}^2$  for fixed  $m_b$ ; right:  $m_b = (4.80 \pm 0.15) \text{ GeV}$  for fixed ratio  $\mu_\pi^2/\bar{\Lambda}^2$ . The data point shows the CLEO measurement.*

the second plot, we vary  $m_b = 4.65 \text{ GeV}$  (long-dashed curve),  $4.8 \text{ GeV}$  (solid curve), and  $4.95 \text{ GeV}$  (short-dashed curve), adjusting the parameter  $\mu_\pi^2$  in such a way that the ratio  $\mu_\pi^2/\bar{\Lambda}^2$  remains fixed. For comparison, we show the data point  $B(B \rightarrow X_s\gamma) = (1.90 \pm 0.47 \pm 0.25) \times 10^{-4}$  obtained by the CLEO Collaboration with a cutoff at  $2.2 \text{ GeV}$  [32]. The fact that in the CLEO analysis the cutoff is imposed on the photon energy in the laboratory frame rather than in the rest frame of the  $B$  meson is not very important for the partially integrated branching ratio [28] and will be neglected here. Obviously, there is a rather strong dependence of the partially integrated branching ratio on the value of the  $b$ -quark mass. In particular, by choosing a low value of  $m_b$  it is possible to get agreement with the CLEO measurement without changing the prediction for the total branching ratio. The important lesson from this investigation is that the theoretical uncertainty in the prediction for the integral over the high-energy part of the photon spectrum is significantly larger than the uncertainty in the prediction of the total branching ratio. So far, this fact has not been taken into account in the comparison of the extrapolated experimental numbers for the total branching ratio with theory. Ultimately, the theoretical errors may be reduced by tuning the parameters of the shape function to fit the measured energy spectrum; however, at present the experimental errors are too large to make such a fit meaningful [28]. Below, we shall perform our calculations for the case  $\delta = 0.3$  corresponding to  $E_\gamma^{\min} \approx 1.85 \text{ GeV}$ , which is large enough to be realistic for near-future experiments, yet low enough to be sufficiently insensitive to the modeling of Fermi motion. As we have pointed out before, the results for the CP asymmetry depend very little on the choice of cutoff.

---

$m_B/2 \approx 2.64 \text{ GeV}$ . Close to the endpoint, our theoretical prediction is “dual” to the true spectrum in an average sense.

## 4 CP asymmetry beyond the Standard Model

In order to explore the implications of various New Physics scenarios for the CP asymmetry and branching ratio in  $B \rightarrow X_s \gamma$  decays it is useful to express the Wilson coefficients  $C_7 = C_7^{\text{eff}}(m_b)$  and  $C_8 = C_8^{\text{eff}}(m_b)$ , which are defined at the scale  $m_b$ , in terms of their values at the high scale  $m_W$ . Using the leading-order renormalization-group equations, one obtains

$$\begin{aligned} C_7 &= \eta^{\frac{16}{23}} C_7(m_W) + \frac{8}{3} \left( \eta^{\frac{14}{23}} - \eta^{\frac{16}{23}} \right) C_8(m_W) + \sum_{i=1}^8 h_i \eta^{a_i}, \\ C_8 &= \eta^{\frac{14}{23}} C_8(m_W) + \sum_{i=1}^8 \bar{h}_i \eta^{a_i}, \end{aligned} \quad (19)$$

where  $\eta = \alpha_s(m_W)/\alpha_s(m_b) \approx 0.56$ , and  $h_i$ ,  $\bar{h}_i$  and  $a_i$  are known numerical coefficients [38]. For the Wilson coefficients at the scale  $m_W$ , we write

$$\begin{aligned} C_7(m_W) &= -\frac{1}{2} A(x_t) + C_7^{\text{new}}(m_W), \\ C_8(m_W) &= -\frac{1}{2} D(x_t) + C_8^{\text{new}}(m_W), \end{aligned} \quad (20)$$

where the first terms correspond to the leading-order Standard Model contributions [39]. They are known functions of the mass ratio  $x_t = (\overline{m}_t(m_W)/m_W)^2$ , which we evaluate with  $\overline{m}_t(m_W) \approx 178 \text{ GeV}$  (corresponding to a pole mass of 175 GeV). This yields  $\frac{1}{2}A(x_t) \approx 0.20$  and  $\frac{1}{2}D(x_t) \approx 0.10$ . Using a similar evolution equation for the next-to-leading coefficient  $C_7^{(1)}$  [33], we find<sup>3</sup>

$$\begin{aligned} C_7 &\approx -0.31 + 0.67 C_7^{\text{new}}(m_W) + 0.09 C_8^{\text{new}}(m_W), \\ C_8 &\approx -0.15 + 0.70 C_8^{\text{new}}(m_W), \\ C_7^{(1)} &\approx -0.48 - 2.29 C_7^{\text{new}}(m_W) - 0.12 C_8^{\text{new}}(m_W). \end{aligned} \quad (21)$$

Below, we will parametrize our results in terms of the magnitude and phase of one of the New Physics contributions,  $C_8^{\text{new}}(m_W) \equiv K_8 e^{i\gamma_8}$  or  $C_7^{\text{new}}(m_W) \equiv -K_7 e^{i\gamma_7}$ , as well as the ratio

$$\xi = \frac{C_7^{\text{new}}(m_W)}{Q_d C_8^{\text{new}}(m_W)}, \quad (22)$$

where  $Q_d = -\frac{1}{3}$ . A given New Physics scenario will make predictions for these quantities at some large scale  $M$ . Using the renormalization group, it is then possible to evolve

---

<sup>3</sup>For consistency, the New Physics contributions entering the expression for  $C_7$  should be taken at next-to-leading order in  $\alpha_s(m_W)$ , i.e., in the radiative decay width the corresponding next-to-leading order New Physics matching corrections would be accounted for through  $C_7$  rather than  $C_7^{(1)}$ .

Table 3: *Ranges of  $\xi(M)$  for various New Physics contributions to  $C_7$  and  $C_8$ , characterized by the particles in penguin diagrams*

Class-1 models	$\xi(M)$	Class-2 models	$\xi(M)$
neutral scalar–quark	1	scalar diquark–top	4.8–8.3
gluino–squark ( $m_{\tilde{g}} < 1.37m_{\tilde{q}}$ )	–(0.13–1)	gluino–squark ( $m_{\tilde{g}} > 1.37m_{\tilde{q}}$ )	–(1–2.9)
techniscalar	$\approx -0.5$	charged Higgs–top	–(2.4–3.8)
		left–right $W$ –top	$\approx -6.7$
		Higgsino–stop	–(2.6–24)

these predictions down to the scale  $m_W$ . At leading order, the analogues of the relations (19) imply

$$\xi \equiv \xi(m_W) = r \xi(M) - 8(1 - r), \quad C_8^{\text{new}}(m_W) = r^7 C_8^{\text{new}}(M), \quad (23)$$

where  $r = [\alpha_s(M)/\alpha_s(m_W)]^{2/3b}$ . Here  $b = 11 - \frac{2}{3}n_f - 2n_g$  is the first  $\beta$ -function coefficient,  $n_f = 6$  is the number of light (with respect to the scale  $M$ ) quark flavours, and  $n_g = 0, 1$  denotes the number of light gluinos. For the purpose of illustration, let us consider the three values  $M = 250$  GeV, 1 TeV and 2.5 TeV, which span a reasonable range of possible New Physics scales. We find

$$\begin{aligned} \xi &\approx 0.98 \xi(250 \text{ GeV}) - 0.12 - 0.03n_g \\ &\approx 0.97 \xi(1 \text{ TeV}) - 0.23 - 0.03n_g \\ &\approx 0.96 \xi(2.5 \text{ TeV}) - 0.29 - 0.04n_g, \end{aligned} \quad (24)$$

i.e.  $\xi$  tends to be smaller than  $\xi(M)$  by an amount of order  $-0.1$  to  $-0.3$  depending on how close the New Physics is to the electroweak scale. These relations will be useful for the discussion below.

For simplicity, we shall restrict ourselves to cases where the parameter  $\xi$  in (22) is real. (Otherwise there would be even more potential for CP violation.) This happens if there is a single dominant New Physics contribution, such as the virtual exchange of a new heavy particle, contributing to both the magnetic and the chromo-magnetic dipole operators. Ranges of  $\xi(M)$  for several illustrative New Physics scenarios are collected in Table 3. They have been obtained, for simplicity, at leading order in  $\alpha_s$  and at the New Physics scale  $M$  characteristic of each particular model. With the help of the relations in (24), the values of  $\xi(M)$  can be translated into the corresponding values of  $\xi$ , which enter our theoretical expressions. Our aim here is not to carry out a detailed study of each model, but to give the reader an idea of the sizable variation that is possible in  $\xi$ . It is instructive to distinguish two classes of models: those with moderate (class-1) and those with large (class-2) values of  $|\xi|$ . It follows from (21) that for small positive values

of  $\xi$  it is possible to have large complex contributions to  $C_8$  without affecting too much the magnitude and phase of  $C_7$ , since

$$\frac{C_8}{C_7} \approx \frac{0.70K_8 e^{i\gamma_8} - 0.15}{(0.09 - 0.22\xi)K_8 e^{i\gamma_8} - 0.31}. \quad (25)$$

This is also true for small negative values of  $\xi$ , albeit over a smaller region of parameter space. New Physics scenarios that have this property belong to class-1 and have been explored in Ref. [19]. They allow for large CP asymmetries resulting from the  $C_7$ – $C_8$  interference term in (12). Examples are penguin diagrams containing new neutral scalars and vector-like quarks with charge  $Q_d = -\frac{1}{3}$ , for which  $\xi(M) = 1$  and hence  $\xi \approx 0.8$ , and supersymmetric penguins containing light gluinos and squarks, for which  $\xi$  is negative and can be tuned by adjusting the mass ratio  $m_{\tilde{q}}/m_{\tilde{q}}$ . A detailed analysis of the decays  $B \rightarrow X_s \gamma$  in the latter scenario is given in Ref. [20] for the case of real  $C_7$  and  $C_8$ . In the table, we specifically consider graphs with flavor off-diagonal left–right down-squark mass insertions under the assumption that the squark masses are approximately degenerate. The gluino and squark masses are taken to lie in the intervals  $150 \text{ GeV} \leq m_{\tilde{q}} \leq 2.5 \text{ TeV}$  and  $250 \text{ GeV} \leq m_{\tilde{q}} \leq 2.5 \text{ TeV}$ , respectively. Another example is provided by models with techniscalars of charge  $\frac{1}{6}$  [19, 40, 41], which have  $\xi(M) \approx -0.5$  and hence  $\xi \approx -0.7$ . In class-1 models, the magnitude of  $C_8$  can be made almost an order of magnitude larger than in the Standard Model without spoiling the theoretical prediction for the  $B \rightarrow X_s \gamma$  branching ratio.

In Figure 3, we show contour plots for the CP asymmetry in the  $(K_8, \gamma_8)$  plane for six different choices of  $\xi$  between  $\frac{3}{2}$  and  $-1$ , assuming a cutoff  $E_\gamma > 1.85 \text{ GeV}$  on the photon energy (corresponding to  $\delta = 0.3$ ). We repeat that the results for the CP asymmetry depend very little on the choice of the cutoff. For each value of  $\xi$ , the plots cover the region  $0 \leq K_8 \leq 2$  and  $0 \leq \gamma_8 \leq \pi$  (changing the sign of  $\gamma_8$  would only change the sign of the CP asymmetry). The contour lines refer to values of the asymmetry of 1%, 5%, 10%, 15% etc. The thick dashed lines indicate contours where the branching ratio takes values between  $1 \times 10^{-4}$  and  $4 \times 10^{-4}$ , as indicated by the numbers inside the squares. For comparison, we recall that the Standard Model prediction with this choice of  $\delta$  is close to  $3.5 \times 10^{-4}$ , whereas the current experimental values are around  $2.5 \times 10^{-4}$ . The main conclusion to be drawn from Figure 3 is that in class-1 scenarios there exists great potential for sizable CP asymmetries in a large region of parameter space. Any point to the right of the 1% contour for  $A_{\text{CP}}^{b \rightarrow s\gamma}$  cannot be accommodated by the Standard Model. On the other hand, we see that asymmetries of several tens of percent<sup>4</sup> are possible in certain extensions of the Standard Model. It is remarkable that in all cases the regions of parameter space that yield the largest values for the CP asymmetries are not excluded by the experimental constraint on the CP-averaged branching ratio. This is because to have large CP asymmetries the cross-products  $C_i C_j^*$  in (12) are required to have large imaginary parts, whereas the total branching ratio is sensitive to the real parts of these quantities. Note, in this context, that the cutoff imposed on the photon energy

---

<sup>4</sup>We show contours only until values  $A_{\text{CP}} = 50\%$ ; for larger values, the theoretical expression for the CP asymmetry in (12) would have to be extended to higher orders to get a reliable result.

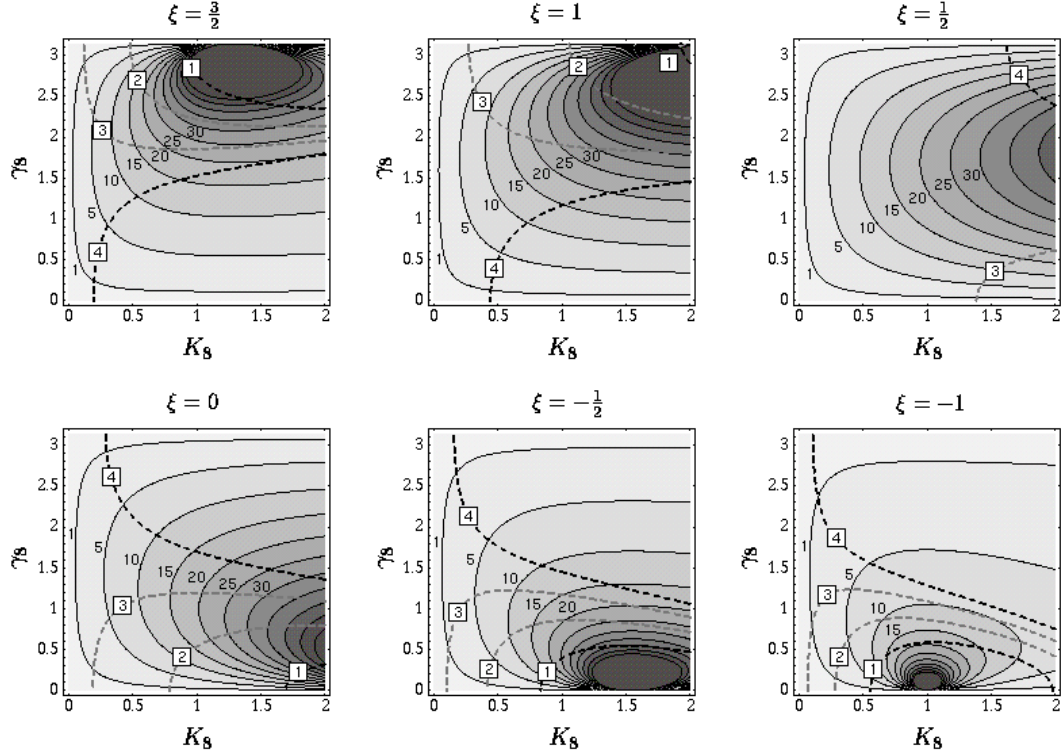


Figure 3: Contour plots for the CP asymmetry  $A_{\text{CP}}^{b \rightarrow s\gamma}$  for various class-1 models

strongly reduces the size of the coefficient of the potentially dangerous term proportional to  $|C_8|^2$  in (18) and thereby helps in keeping the prediction for the branching ratio at an acceptably low level even for large values of  $K_8$ .

There are also scenarios in which the parameter  $\xi$  takes on larger negative or positive values. In such cases, it is not possible to increase the magnitude of  $C_8$  much over its Standard Model value, and the only way to get large CP asymmetries from the  $C_7$ – $C_8$  or  $C_7$ – $C_2$  interference terms in (12) is to have  $C_7$  tuned to be very small; however, this possibility is constrained by the fact that the total  $B \rightarrow X_s\gamma$  branching ratio must be of an acceptable magnitude. That this condition starts to become a limiting factor is already seen in the plots corresponding to  $\xi = -\frac{1}{2}$  and  $-1$  in Figure 3. For even larger values of  $|\xi|$ , the  $C_7$ – $C_8$  interference term becomes ineffective, because the weak phase tends to cancel in the ratio  $C_8/C_7$  in (25). Then the  $C_2$ – $C_7$  interference term becomes the main source of CP violation; however, as discussed in Section 2, it cannot lead to asymmetries exceeding a level of about 5% without violating the constraint that the  $B \rightarrow X_s\gamma$  branching ratio not be too small. Models of this type belong to the class-2 category. Some examples are listed in the right portion of Table 3 and can be summarized as follows.

Models with gluino–squark loops can have large negative  $\xi$  if the ratio  $m_{\tilde{g}}/m_{\tilde{q}}$  is sufficiently large. Penguin graphs in left–right symmetric models with right-handed couplings of the  $W$  boson to the top and bottom quarks and internal top-mass chirality

flip have  $\xi(M) \approx \xi \approx -6.7$ . Charged-Higgs–top penguins in multi-Higgs models always have  $\xi(M) < -2$  because of the charge of the top quark. In the table graphs with internal chirality flip are considered, with charged Higgs mass lying in the range  $125 \text{ GeV} \leq m_{H^-} \leq 2.5 \text{ TeV}$  (where  $\xi$  increases as  $m_{H^-}$  is increased). In general multi-Higgs models these graphs are enhanced by a power of  $m_t/m_b$  relative to their counterparts with external chirality flip. Examples are type-3 two-Higgs-doublet models [22], left–right symmetric models [23], [42]–[44], or models with additional Higgs doublets which do not acquire significant vacuum expectation values. In all of these examples new CP-violating phases can enter the penguin graphs, unlike in type-2 two-Higgs doublet models. Chargino–stop penguins always lead to sizable negative values of  $\xi$ . For simplicity, we have considered loops that contain a pure charged Higgsino which flips chirality. The superpartners of new Higgs doublets with negligible vacuum expectation values would, for example, be pure Higgsinos. The physical stop and Higgsino masses are varied in the ranges  $175 \text{ GeV} \lesssim m_{\tilde{t}_1}, m_{\tilde{t}_2} \lesssim 2.5 \text{ TeV}$  and  $125 \text{ GeV} \leq m_{\tilde{h}} \leq 2.5 \text{ TeV}$ , respectively, under the simplifying assumption that the stop mass matrix has equal diagonal entries,  $m^2$ , and equal off-diagonal (left–right) entries,  $\mu^2$ , with magnitudes satisfying  $|\mu|^2 \leq |mm_t|$ . Finally, large positive values of  $\xi$  arise from penguin graphs with a charge  $-\frac{1}{3}$  scalar “diquark” and anti-top quark in the loop. The range of values for  $\xi(M)$  quoted is again obtained for graphs with internal chirality flip, and scalar diquark mass in the range  $250 \text{ GeV}–2.5 \text{ TeV}$  (where  $\xi$  decreases as the scalar mass increases). In general, the phase structure of new penguin contributions with internal and external chirality flip will differ in the above examples; however, since the former tend to dominate due to chiral enhancement of order  $m_F/m_b$ , where  $m_F$  is the mass of the heavy fermion in the loop,  $\xi$  will be real to good approximation.

For a graphical analysis of class-2 models it is convenient to choose the magnitude and phase of the new-physics contribution  $C_7^{\text{new}}(m_W) \equiv -K_7 e^{i\gamma_7}$  as parameters, rather than  $K_8$  and  $\gamma_8$ . The reason is that for large  $|\xi|$  it becomes increasingly unlikely that  $C_8^{\text{new}}(m_W)$  will be large. The resulting plots are given in Figure 4. As before, the dashed lines indicate the acceptable range for the  $B \rightarrow X_s \gamma$  branching ratio. The branching-ratio constraint allows larger values of  $C_8$  for positive  $\xi$ , which explains why larger asymmetries are attainable in this case. For example, for  $\xi \approx 5$ , which can be obtained from scalar diquark–top penguins, asymmetries of 5–20% are seen to be consistent with the  $B \rightarrow X_s \gamma$  bound. On the other hand, for  $\xi \approx -(2.5–5)$ , which includes the multi-Higgs-doublet models, CP asymmetries of only a few percent are attainable, in agreement with the findings of previous authors [22, 23, 45]. The same is true for the left–right symmetric  $W$ –top penguin, particularly if one takes into account that  $K_7 \lesssim 0.2$  if  $m_{W_R} > 1 \text{ TeV}$ .

The New Physics scenarios explored in Figure 3 have the attractive feature of a possible large enhancement of the magnitude of the Wilson coefficient  $C_8$ . This has important implications for the phenomenology of the semileptonic branching ratio and charm production yield in  $B$  decays, through enhanced production of charmless hadronic final states induced by the  $b \rightarrow sg$  flavour-changing neutral current (FCNC) transition [19, 20, 46]. At  $O(\alpha_s)$ , the theoretical expression for the  $B \rightarrow X_{sg}$  decay rate is obtained

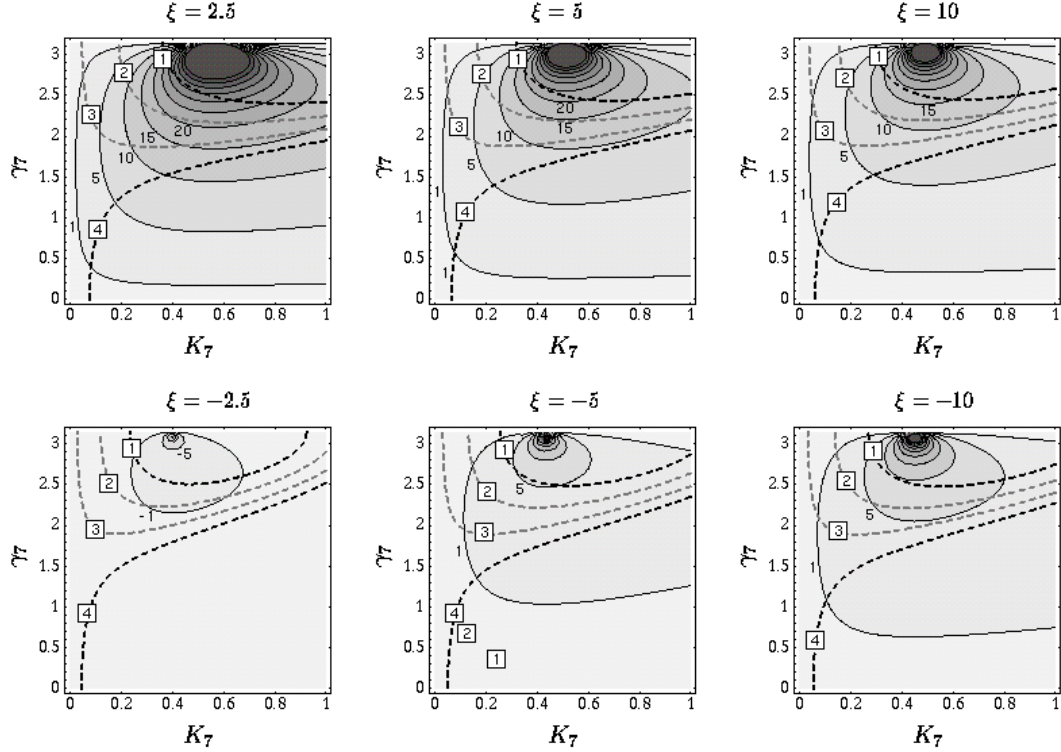


Figure 4: Contour plots for the  $CP$  asymmetry  $A_{CP}^{b \rightarrow s \gamma}$  for various class-2 models

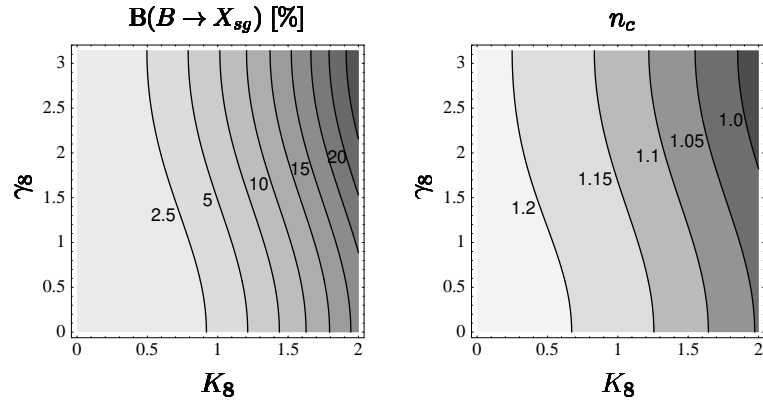


Figure 5:  $B \rightarrow X_{sg}$  branching ratio (left) and charm yield in  $B$  decays (right) as a function of the parameters  $K_8$  and  $\gamma_8$ . There is an overall theoretical uncertainty of 6% on the values of  $n_c$ .

from obvious substitutions in (6) to be

$$\Gamma(B \rightarrow X_{sg}) = \frac{G_F^2 m_b^5 \alpha_s(m_b)}{24\pi^4} |v_t C_8|^2. \quad (26)$$

Normalizing this to the semileptonic rate, we obtain for the corresponding branching ratio  $B(B \rightarrow X_{sg}) \approx 0.96 |C_8|^2 \times B(B \rightarrow X_c e \bar{\nu})$ . In the first plot in Figure 5, we show contours for the  $B \rightarrow X_{sg}$  branching ratio, normalized to  $B(B \rightarrow X_c e \bar{\nu}) = 10.5\%$ , in the  $(K_8, \gamma_8)$  plane. In the Standard Model,  $B(B \rightarrow X_{sg}) \approx 0.2\%$  is very small; however, in scenarios with  $|C_8| = O(1)$  sizable values of order 10% for this branching ratio are possible, which simultaneously lowers the theoretical predictions for the semileptonic branching ratio and the charm production rate  $n_c$  by a factor of  $[1 + B(B \rightarrow X_{sg})]^{-1}$ . The most recent value of  $n_c$  reported by the CLEO Collaboration is  $1.12 \pm 0.05$  [34]. Although the systematic errors in this measurement are large, the result favours values of  $B(B \rightarrow X_{sg})$  of order 10% [47]. This is apparent from the second plot in Figure 5, where we show the central theoretical prediction for  $n_c$  as a function of  $K_8$  and  $\gamma_8$ . (There is an overall theoretical uncertainty in the value of  $n_c$  of about 6% [48], resulting from the dependence on quark masses and the renormalization scale.) The theoretical prediction for the semileptonic branching ratio would have the same dependence on  $K_8$  and  $\gamma_8$ , with the normalization  $B_{SL} = (12 \pm 1)\%$  fixed at  $K_8 = 0$  [48]. A large value of  $B(B \rightarrow X_{sg})$  could also help in understanding the  $\eta'$  yields in charmless  $B$  decays [49, 50]. For completeness, we note that the CLEO Collaboration has recently presented a preliminary upper limit<sup>5</sup> on  $B(B \rightarrow X_{sg})$  of 6.8% (90% CL) [53]. It is therefore worth noting that large CP asymmetries of order 10–20% are easily attained at smaller  $B \rightarrow X_{sg}$  branching ratios of a few percent, which would nevertheless represent a marked departure from the Standard Model prediction.

## 5 Dipole operators with right-handed light quarks, and models without CKM unitarity

All the models listed in Table 3 can have non-standard dipole operators involving right-handed light-quark fields. In fact, in the absence of horizontal symmetries which impose special hierarchies among the model parameters there is no reason why these should be any less important than the operators of the standard basis. We therefore briefly discuss modifications to our previous analysis in their presence. Denoting by  $C_7^R$  and  $C_8^R$  the Wilson coefficients multiplying the new operators, the expressions (12), (18) and (26) must be modified by replacing  $C_i C_j^* \rightarrow C_i C_j^* + C_i^R C_j^{R*}$  everywhere, taking however into account that  $C_2^R = 0$ . Note that for a single dominant New Physics contribution the parametrization in (22) for the standard dipole operators will also be valid for the new operators, with  $\xi$  taking the same real value. Then the only change in the prediction for

---

<sup>5</sup>The limit is increased to 8.9% if one uses the more recent charmed baryon and charmonium yields presented in Refs. [34, 51] and makes use of the relative  $\Lambda_c$  versus  $\bar{\Lambda}_c$  yields given in Ref. [52].

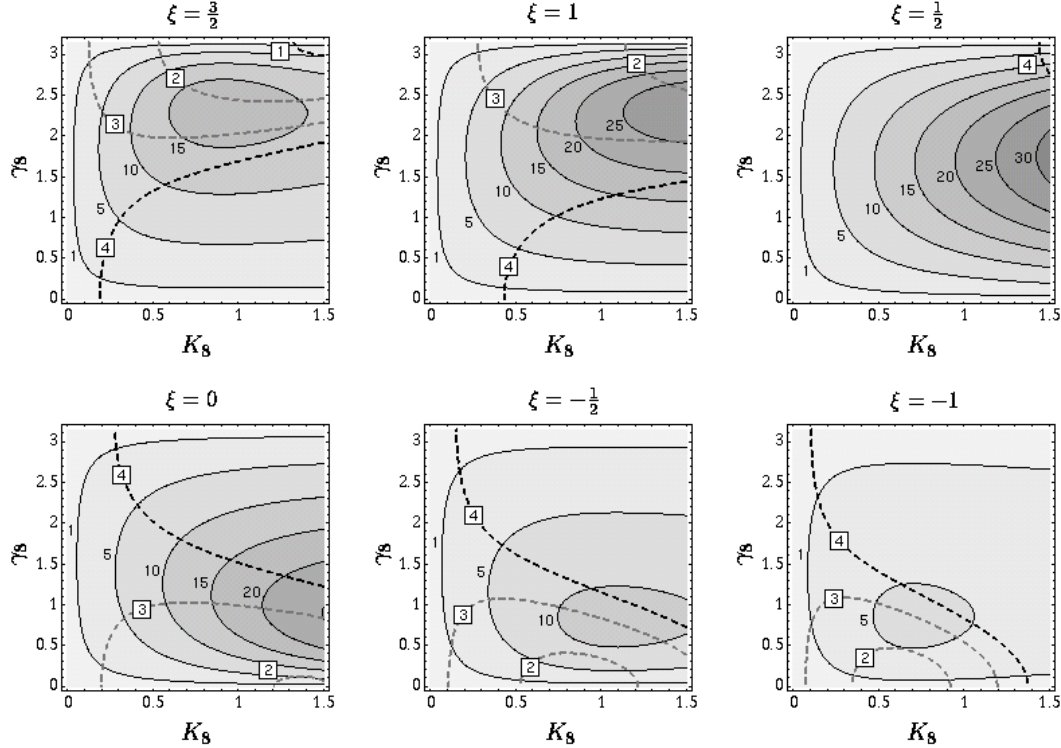


Figure 6: Contour plots for the CP asymmetry  $A_{\text{CP}}^{b \rightarrow s\gamma}$  for the same choices of the parameter  $\xi$  as in Figure 3, but including the effect of different-chirality operators (as explained in the text)

the CP asymmetry is that in the denominator of (12) the coefficient  $|C_7|^2$  is replaced by  $|C_7|^2 + |C_7^R|^2$ . On the other hand, there are several new contributions to the prediction for the total  $B \rightarrow X_s \gamma$  branching ratio, as can be seen from (18). For the purpose of illustration, let us assume that the New Physics contributions are the same for operators of different chirality, i.e.  $C_i^{R,\text{new}}(m_W) = C_i^{\text{new}}(m_W)$  for  $i = 7, 8$ . The results are shown in Figure 6, where we explore the same range of  $\xi$  values as in Figure 3. The predictions for the  $B \rightarrow X_{sg}$  branching ratio are enhanced because  $|C_8|^2$  in (26) is replaced by  $|C_8|^2 + |C_8^R|^2$ , so we only consider the range  $0 \leq K_8 \leq 1.5$ , which covers the same values of  $B(B \rightarrow X_{sg})$  as before. Comparing Figures 3 and 6, we observe that although there is a clear dilution of the resulting CP asymmetries caused by the inclusion of opposite-chirality operators, there is still plenty of parameter space in which the asymmetries are much larger than in the Standard Model. We should also point out that, if there is more than one significant New Physics contribution to the dipole operators, there need not be any dilution since the product  $C_8^R C_7^{R*}$  could develop an imaginary part, thus providing an additional contribution to the CP asymmetry.

Finally, we briefly discuss what happens in models with CKM unitarity violation. In terms of the quantity  $\Delta_s$  defined by  $v_u + v_c + (1 + \Delta_s)v_t = 0$ , the result for the CP

asymmetry in (7) generalizes to

$$\begin{aligned}
A_{\text{CP}}^{b \rightarrow s\gamma}(\delta) &= \frac{\Gamma(\bar{B} \rightarrow X_s \gamma) - \Gamma(B \rightarrow X_{\bar{s}} \gamma)}{\Gamma(\bar{B} \rightarrow X_s \gamma) + \Gamma(B \rightarrow X_{\bar{s}} \gamma)} \Big|_{E_\gamma > (1-\delta)E_\gamma^{\text{max}}} \\
&= \frac{\alpha_s(m_b)}{|C_7|^2} \left\{ \frac{40}{81} \text{Im}[(1 + \Delta_s)C_2 C_7^*] - \frac{8z}{9} [v(z) + b(z, \delta)] \text{Im}[(1 + \epsilon_s + \Delta_s)C_2 C_7^*] \right. \\
&\quad \left. - \frac{4}{9} \text{Im}[C_8 C_7^*] + \frac{8z}{27} b(z, \delta) \text{Im}[(1 + \epsilon_s + \Delta_s)C_2 C_8^*] \right\}. \quad (27)
\end{aligned}$$

$\Delta_s$  parametrizes the deviation from unitarity of the 3-generation CKM matrix, which could be caused, for instance, by mixing of the known down quarks with a new isosinglet heavy quark, or by the existence of a sequential fourth generation of quarks. In principle, asymmetries much larger than in the Standard Model could be attained provided that  $\Delta_s$  has a significant weak phase. This reflects the fact that the GIM suppression is no longer at work if CKM unitarity is violated. However, we will now show that in plausible scenarios the effect of  $\Delta_s$  on the CP asymmetry is very small. In the case of mixing with isosinglets, existing experimental limits [54] on the FCNC process  $B \rightarrow X_s \ell^+ \ell^-$  induced by tree-level  $Z$  exchange [55] imply  $\Delta_s < 0.04$ . The impact of non-unitarity can therefore be safely neglected, since new contributions to the CP asymmetry would be well below 1%. Let us, therefore, turn to the case of a sequential fourth generation with a new up-type quark denoted by  $t'$ . As before, we will neglect the small quantity  $\epsilon_s$ , so that  $\text{Im}[\Delta_s]$  is the only source of CP violation. Then the above expression can be rewritten in the simpler form

$$A_{\text{CP}}^{b \rightarrow s\gamma}(\delta) = a_{27}(\delta) \text{Im} \left[ \frac{(1 + \Delta_s)C_2}{C_7} \right] + a_{87} \text{Im} \left[ \frac{C_8}{C_7} \right] + a_{28}(\delta) \text{Im} \left[ \frac{(1 + \Delta_s)C_2}{C_7} \cdot \frac{C_8^*}{C_7^*} \right]. \quad (28)$$

In such a scenario, the CP asymmetry is affected not only by the non-unitarity of the 3-generation CKM matrix with  $\Delta_s = v_{t'}/v_t$  in (27), but also by the new contributions of the  $t'$  quark to the Wilson coefficients  $C_7$  and  $C_8$  at the scale  $m_W$ . In analogy with (20), we have

$$C_7(m_W) = -\frac{1}{2} [A(x_t) + \Delta_s A(x_{t'})], \quad C_8(m_W) = -\frac{1}{2} [D(x_t) + \Delta_s D(x_{t'})], \quad (29)$$

where  $x_{t'} = (\bar{m}_{t'}(m_W)/m_W)^2$ . In addition, there is a modification to the evolution equations (19) for the Wilson coefficients  $C_7$  and  $C_8$ , where now the last terms (those involving the coefficients  $h_i$  and  $\bar{h}_i$ ) must be multiplied by  $-(v_c + v_u)/v_t = (1 + \Delta_s)$ . Taking  $m_{t'} = 250$  GeV for the purpose of illustration, we obtain  $C_7 \approx -0.31 - 0.34\Delta_s$  and  $C_8 \approx -0.15 - 0.16\Delta_s$ , i.e. to a good approximation we have  $C_{7,8} \approx (1 + \Delta_s)C_{7,8}^{\text{SM}}$ . This just reflects the fact that the functions  $A(x)$  and  $D(x)$  are slowly varying for  $x \gg 1$ . In this limit, however, all dependence on  $\Delta_s$  cancels in the expression for the CP asymmetry. As a result, there is in general not much potential for having large CP asymmetries in models with a sequential fourth generation. For all realistic choices of parameters, we find asymmetries of less than 2%, i.e. of a similar magnitude as in the Standard Model.

## 6 Conclusions

We have presented a study of direct CP violation in the inclusive, radiative decays  $B \rightarrow X_s \gamma$ . From a theoretical point of view, inclusive decay rates entail the advantage of being calculable in QCD, so that a reliable prediction for the CP asymmetry can be confronted with data. From a practical point of view, it is encouraging that the rare radiative decays of  $B$  mesons have already been observed experimentally, and high-statistics measurements of the corresponding rates will be possible in the near future. We find that in the Standard Model the CP asymmetry in  $B \rightarrow X_s \gamma$  decays is strongly suppressed by three small parameters:  $\alpha_s(m_b)$  arising from the necessity of having strong phases,  $\sin^2\theta_C \approx 5\%$  reflecting a CKM suppression, and  $(m_c/m_b)^2 \approx 8\%$  resulting from a GIM suppression. As a result, the CP asymmetry can be safely predicted to lie below 1% in magnitude. We have argued that the latter two suppression factors are inoperative in extensions of the Standard Model for which the effective Wilson coefficients  $C_7$  and  $C_8$  receive additional contributions involving non-trivial weak phases. Much larger CP asymmetries of  $O(\alpha_s)$  are therefore possible in such cases.

We have presented a model-independent analysis of New Physics scenarios in terms of the magnitudes and phases of the Wilson coefficients  $C_7$  and  $C_8$ , finding that, indeed, sizable CP asymmetries are predicted in large regions of parameter space. Some explicit realizations of models with large CP asymmetries have been illustrated. In particular, we have shown that asymmetries of 10–50% are possible in models which allow for a strong enhancement of the contribution from the chromo-magnetic dipole operator. This is, in fact, quite natural unless there is a symmetry that forbids new weak phases from entering the coefficients  $C_7$  and  $C_8$ . We have also shown that the predictions for the CP asymmetry are only moderately diluted if operators involving right-handed light-quark fields are included in the analysis. On the other hand, we confirm the findings of previous authors regarding the smallness of the CP asymmetry that is attainable in two-Higgs-doublet models and in left-right symmetric models. Moreover, we find very small effects for models in which 3-generation unitarity is violated. Quite generally, having a large CP asymmetry is not in conflict with the observed value for the CP-averaged  $B \rightarrow X_s \gamma$  branching ratio. On the contrary, it may even help to lower the theoretical prediction for this quantity, and likewise for the semileptonic branching ratio and charm multiplicity in  $B$  decays, thereby bringing these three observables closer to their experimental values.

The fact that a large inclusive CP asymmetry in  $B \rightarrow X_s \gamma$  decays is possible in many generic extensions of the Standard Model, and in a large region of parameter space, offers the exciting possibility of looking for a signature of New Physics in these decays using data sets that will become available during the first period of operation of the  $B$  factories (if not existing data sets). A negative result of such a study would impose constraints on many New Physics scenarios. A large positive signal, on the other hand, would provide interesting clues about the nature of physics beyond the Standard Model. In particular, a CP asymmetry exceeding the level of 10% would be a strong hint towards enhanced chromo-magnetic dipole transitions caused by some new flavour physics at a high scale.

We have restricted our analysis to the case of inclusive radiative decays since they

entail the advantage of being very clean, in the sense that the strong-interaction phases relevant for direct CP violation can be reliably calculated. However, if there is New Physics that induces a large inclusive CP asymmetry in  $B \rightarrow X_s \gamma$  decays, it will inevitably also lead to sizable asymmetries in some related processes. In particular, since we found that the inclusive CP asymmetry remains almost unaffected if a cut on the high-energy part of the photon energy spectrum is imposed, we expect that a large asymmetry will persist in the exclusive mode  $B \rightarrow K^* \gamma$ , even though a reliable theoretical analysis would be much more difficult because of the necessity of calculating final-state rescattering phases [56]. Still, it is worthwhile searching for a large CP asymmetry in this channel.

Finally, it has been shown in Ref. [57] that New Physics can lead to a large time-dependent CP asymmetry in exclusive  $B^0 \rightarrow K^{*0} \gamma$  decays through interference of mixing and decay. Large direct CP violation would introduce hadronic uncertainties, thus complicating the analysis of this effect. However, it is interesting to note that the two phenomena are in a sense complementary in that to a large extent they probe different New Physics contributions. We have seen that direct CP asymmetries in radiative  $B$  decays are primarily sensitive to modifications of the Wilson coefficients of the dipole operators with standard chirality. On the other hand, the presence of dipole operators with right-handed light-quark fields, which are of negligible strength in the Standard Model, is crucial for obtaining time-dependent asymmetries, since these require both the  $B^0$  and  $\bar{B}^0$  to be able to decay to states with the same photon helicity.

*Acknowledgments:* We would like to thank Andrzej Buras, Lance Dixon, Gian Giudice, Laurent Lellouch, Mikolaj Misiak, Yossi Nir and Mike Sokoloff for helpful discussions. We are indebted to Persis Drell and Steven Glenn for discussing aspects of the CLEO measurement of the  $B \rightarrow X_s \gamma$  branching ratio. One of us (A.K.) would like to thank the CERN Theory group for its hospitality during part of this work. A.K. was supported by the United States Department of Energy under Grant No. DE-FG02-84ER40153.

## References

- [1] J.M. Gérard and J. Weyers, Preprint UCL-IPT-97-18 [hep-ph/9711469].
- [2] M. Neubert, Preprint CERN-TH/97-342 [hep-ph/9712224].
- [3] A.F. Falk, A.L. Kagan, Y. Nir and A.A. Petrov, Preprint JHU-TIPAC-97018 [hep-ph/9712225].
- [4] D. Atwood and A. Soni, Preprint [hep-ph/9712287].
- [5] For a review, see: R. Fleischer, Int. J. Mod. Phys. A **12**, 2459 (1997).
- [6] J. Chay, H. Georgi and B. Grinstein, Phys. Lett. B **247**, 399 (1990).

- [7] I.I. Bigi, N.G. Uraltsev and A.I. Vainshtein, Phys. Lett. B **293**, 430 (1992) [E: **297**, 477 (1993)]; I.I. Bigi, M.A. Shifman, N.G. Uraltsev and A.I. Vainshtein, Phys. Rev. Lett. **71**, 496 (1993); B. Blok, L. Koprakh, M.A. Shifman and A.I. Vainshtein, Phys. Rev. D **49**, 3356 (1994) [E: **50**, 3572 (1994)].
- [8] A.V. Manohar and M.B. Wise, Phys. Rev. D **49**, 1310 (1994).
- [9] M. Beneke, G. Buchalla and I. Dunietz, Phys. Lett. B **393**, 132 (1997).
- [10] A.F. Falk, M. Luke and M.J. Savage, Phys. Rev. D **49**, 3367 (1994).
- [11] M. Neubert, Phys. Rev. D **49**, 3392 and 4623; T. Mannel and M. Neubert, Phys. Rev. D **50**, 2037 (1994).
- [12] I.I. Bigi, M.A. Shifman, N.G. Uraltsev and A.I. Vainshtein, Int. J. Mod. Phys. A **9**, 2467 (1994); R.D. Dikeman, M. Shifman and N.G. Uraltsev, Int. J. Mod. Phys. A **11**, 571 (1996).
- [13] M.B. Voloshin, Phys. Lett. B **397**, 275 (1997).
- [14] A. Khodjamirian, R. Rückl, G. Stoll and D. Wyler, Phys. Lett. B **402**, 167 (1997).
- [15] Z. Ligeti, L. Randall and M.B. Wise, Phys. Lett. B **402**, 178 (1997).
- [16] A.K. Grant, A.G. Morgan, S. Nussinov and R.D. Peccei, Phys. Rev. D **56**, 3151 (1997).
- [17] G. Buchalla, G. Isidori and S.J. Rey, Nucl. Phys. B **511**, 594 (1998).
- [18] For a review, see: G. Buchalla, A.J. Buras and M.E. Lautenbacher, Rev. Mod. Phys. **68**, 1125 (1996).
- [19] A.L. Kagan, Phys. Rev. D **51**, 6196 (1995).
- [20] M. Ciuchini, E. Gabrielli and G.F. Giudice, Phys. Lett. B **388**, 353 (1996) [E: **393**, 489 (1997)].
- [21] J.M. Soares, Nucl. Phys. B **367**, 575 (1991).
- [22] L. Wolfenstein and Y.L. Wu, Phys. Rev. Lett. **73**, 2809 (1994).
- [23] H.M. Asatrian and A.N. Ioannissian, Phys. Rev. D **54**, 5642 (1996); H.M. Asatrian, G.K. Yeghiyan and A.N. Ioannissian, Phys. Lett. B **399**, 303 (1997).
- [24] L.T. Handoko, Phys. Rev. D **57**, 1776 (1998); Preprint HUPD-9714 [hep-ph/9708447].
- [25] M. Bander, D. Silverman and A. Soni, Phys. Rev. Lett. **43**, 242 (1979).

- [26] C. Greub, T. Hurth and D. Wyler, Phys. Lett. B **380**, 385 (1996); Phys. Rev. D **54**, 3350 (1996).
- [27] For a review, see: M. Neubert, Int. J. Mod. Phys. A **11**, 4173 (1996).
- [28] A.L Kagan and M. Neubert, in preparation.
- [29] A.F. Falk and M. Neubert, Phys. Rev. D **47**, 2965 (1993).
- [30] M.S. Alam et al. (CLEO Collaboration), Phys. Rev. Lett. **74**, 2885 (1995).
- [31] P.G. Colrain and M.I. Williams (representing the ALEPH Collaboration), to appear in the Proceedings of the XXXII. Rencontres de Moriond: Electroweak Interactions and Unified Theories, Les Arcs, France, March 1997.
- [32] Steven Glenn, private communication. The correction factor has been calculated using the model of: A. Ali and C. Greub, Phys. Lett. B **259**, 182 (1991).
- [33] K. Chetyrkin, M. Misiak and M. Münz, Phys. Lett. B **400**, 206 (1997).
- [34] P. Drell, Preprint CLNS-97-1521 [hep-ex/9711020], to appear in the Proceedings of the 18th International Symposium on Lepton–Photon Interactions, Hamburg, Germany, July 1997.
- [35] M. Neubert, Preprint CERN-TH/98-2 [hep-ph/9801269], to appear in the Proceedings of the International Europhysics Conference on High Energy Physics, Jerusalem, Israel, August 1997.
- [36] A.J. Buras, A. Kwiatkowski and N. Pott, Phys. Lett. B **414**, 157 (1997).
- [37] M. Ciuchini, G. Degrassi, P. Gambino and G.F. Giudice, Preprint CERN-TH-97-279 [hep-ph/9710335].
- [38] A.J. Buras, M. Misiak, M. Münz and S. Pokorski, Nucl. Phys. B **424**, 374 (1994).
- [39] B. Grinstein, R. Springer and M.B. Wise, Nucl. Phys. B **339**, 269 (1990).
- [40] A.L. Kagan, Proceedings of the 15th Johns Hopkins Workshop on Current Problems in Particle Theory, edited by G. Domokos and S. Kovesi-Domokos (World Scientific, Singapore, 1992), pp. 217.
- [41] B.A. Dobrescu, Nucl. Phys. B **449**, 462 (1995); B.A. Dobrescu and J. Terning, Phys. Lett. B **416**, 129 (1998).
- [42] K.S. Babu, K. Fujikawa and A. Yamada, Phys. Lett. B **333**, 196 (1994).
- [43] P. Cho and M. Misiak, Phys. Rev. D **49**, 5894 (1994).
- [44] T.G. Rizzo, Phys. Rev. D **50**, 3303 (1994).

- [45] F.M. Borzumati and C. Greub, Preprint ZU-TH 31/97 [hep-ph/9802391].
- [46] B.G. Grzadkowski and W.-S. Hou, *Phys. Lett. B* **272**, 383 (1991).
- [47] A.L. Kagan and J. Rathsman, University of Cincinnati Preprint [hep-ph/9701300];  
A.L. Kagan, to appear in the Proceedings of the 2nd International Conference on B Physics and CP Violation, Honolulu, Hawaii, March 1997.
- [48] M. Neubert and C.T. Sachrajda, *Nucl. Phys. B* **438**, 235 (1995).
- [49] W.-S. Hou and B. Tseng, *Phys. Rev. Lett.* **80**, 434 (1998).
- [50] A.L. Kagan and A.A. Petrov, Preprint UCHEP-97/27 [hep-ph/9707354].
- [51] L. Gibbons et al. (CLEO Collaboration), *Phys. Rev. D* **56**, 3783 (1997).
- [52] D. Cinabro et al. (CLEO Collaboration), Conference contribution CLEO-CONF 94-8, submitted to the International Conference on High Energy Physics, Glasgow, Scotland, July 1994.
- [53] T.E. Coan et al. (CLEO Collaboration), Preprint CLNS 97/1516 [hep-ex/9710028].
- [54] S. Glenn et al. (CLEO Collaboration), Preprint CLNS 97/1514 [hep-ex/9710003].
- [55] Y. Nir and D. Silverman, *Phys. Rev. D* **42**, 1477 (1990); D. Silverman, *Phys. Rev. D* **45**, 1800 (1992).
- [56] C. Greub, H. Simma and D. Wyler, *Nucl. Phys. B* **434**, 39 (1995).
- [57] D. Atwood, M. Gronau and A. Soni, *Phys. Rev. Lett.* **79**, 185 (1997).